EARTHQUAKE ENGINEERING AND STRUCTURAL DYNAMICS
Earthquake Engng Struct. Dyn. 2002; **31**:791–812 (DOI: 10.1002/eqe.122)

Tangential-projection algorithm for manifold representation in unidentifiable model updating problems

Lambros S. Katafygiotis*,† and Heung-Fai Lam

Department of Civil and Structural Engineering, Hong Kong University of Science and Technology, Clear Water Bay, Hong Kong

SUMMARY

The problem of updating a structural model and its associated uncertainties by utilizing structural response data is addressed. In an identifiable case, the posterior probability density function (PDF) of the uncertain model parameters for given measured data can be approximated by a weighted sum of Gaussian distributions centered at a number of discrete optimal values of the parameters at which some positive measure-of-fit function is minimized. The present paper focuses on the problem of model updating in the general unidentifiable case for which certain simplifying assumptions available for identifiable cases are not valid. In this case, the PDF is distributed in the neighbourhood of an extended and usually highly complex manifold of the parameter space that cannot be calculated explicitly. The computational difficulties associated with calculating the highly complex posterior PDF are discussed and a new adaptive algorithm, referred to as the tangential-projection (TP) algorithm, allowing for an efficient approximate representation of the above manifold and the posterior PDF is presented. Using this approximation, expressions for calculating the uncertain predictive response are established. A numerical example involving noisy data is presented to demonstrate the proposed method. Copyright © 2002 John Wiley & Sons, Ltd.

KEY WORDS: Bayesian; unidentifiable; model updating; manifold; system identification

1. INTRODUCTION

The need for model updating arises because there are always errors associated with the process of constructing a theoretical model of a structure, which leads to uncertain accuracy in the predictive response. Because of these modeling errors, model updating is best tackled as a statistical inference problem. This can be done by embedding the class of 'deterministic' structural models within a class of probability models so that the structural models give a

* Correspondence to: Lambros S. Katafygiotis, Department of Civil and Structural Engineering, Hong Kong University of Science and Technology, Clear Water Bay, Hong Kong.
† E-mail: lambros@usthk.ust.hk

Contract/grant sponsor: Hong Kong Research Grant Council; contract/grant numbers: HKUST 604/97E and HKUST 6253/00.

Received 27 June 2000
Revised 26 June 2001
Accepted 3 July 2001

predictable ('systematic') part and the prediction error is modeled as an uncertain ('random') part (Reference [1]). Beck and Katafygiotis [2] presented a general Bayesian statistical system identification framework which properly handles the uncertainties and non-uniqueness associated with model updating. Furthermore, they described an asymptotic approximation for the multi-dimensional integrals that arise when calculating the updated probabilistic predictions of the structural response. This approximation is valid for identifiable cases, which usually occur when the number of the updating parameters is relatively small and when the number of observed data is large. In such a case the posterior PDF of the model parameters is very peaked at a finite number of optimal points, at which some positive measure-of-fit function is minimized, and it is practically concentrated in the immediate neighbourhood of these optimal points. In Reference [2] the authors presented an asymptotic approximation for the posterior PDF of the parameters using a finite sum of appropriately weighted Gaussian distributions centered at the optimal points. They also showed that in this case the probability distribution of the predictive response can be asymptotically approximated by a weighted sum of Gaussian distributions centered at the predictive responses of the optimal models. Katafygiotis and Beck [3] presented an algorithm for resolving the problem of model identifiability, that is, given an optimal model, they resolved the problem of finding all other output-equivalent optimal models. Once the set of all optimal models has been computed based on the algorithm in Reference [3], one can readily apply the earlier asymptotic approximations to resolve the model updating problem in a globally or locally identifiable case [2].

The present paper is based on the general Bayesian statistical model updating framework presented in Reference [2]. Herein we address the computational difficulties associated with the implementation of this general methodology in an unidentifiable case, where the asymptotic approximations presented in Reference [2] are not valid. In this case the posterior PDF is concentrated in the neighbourhood of an extended and extremely complex manifold in the parameter space. Analytical representation of this manifold is usually not possible and, therefore, issues related to its numerical calculation and its practical representation arise. Herein a new algorithm, referred to as the tangential-projection (TP) algorithm [4], is proposed for the calculation of a finite set of points on the manifold used for its representation. Specifically, it is proposed that for practical applications the posterior PDF of the model parameters is approximated by a finite number of weighted Dirac delta functions centered at the computed points on the manifold. Furthermore, the PDF of the uncertain predictive response can be approximated by a weighted sum of the PDFs of the predictive responses corresponding to these points.

2. IDENTIFIABLE AND UNIDENTIFIABLE CASES

2.1. Identifiable cases

This work is based on the Bayesian statistical identification framework presented in Beck and Katafygiotis [2]. The methodology allows for the calculation of the posterior PDF of the parameters $\boldsymbol{\alpha}^{\mathrm{T}} = [\mathbf{a}, \sigma]^{\mathrm{T}}$ specifying the various models out of a class of probability models $\mathscr{M}_P$ for the system output; the parameters $\mathbf{a} \in S(\mathbf{a}) \subseteq R^{N_a}$ specify a deterministic model for the predictable part of the structural response while the parameter σ specifies a probability model for the uncertain prediction-error. The posterior PDF of the structural model parameters $\mathbf{a}$

given some measured data $\mathscr{D}_N$ can be calculated [2] as

$$p(\mathbf{a} \mid \mathscr{D}_N, \mathscr{M}_P) = c_1 J(\mathbf{a})^{-N_J} \pi(\mathbf{a}, \hat{\sigma}(\mathbf{a})) \tag{1}$$

where c_1 is a normalizing constant; $N_J = (NN_o - 1)/2$ where N denotes the number of sampled data and N_o the number of observed DOFs; $\pi(\mathbf{a}, \sigma)$ denotes the prior PDF of the parameters; and $\hat{\sigma}(\mathbf{a})$, $J(\mathbf{a})$ are defined as

$$\hat{\sigma}^2(\mathbf{a}) = \frac{1}{N_o N} \sum_{n=1}^{N} \|\hat{\mathbf{y}}(n) - S_o \mathbf{q}(n; \mathbf{a})\|^2 = J(\mathbf{a}) \tag{2}$$

where $\hat{\mathbf{y}}(n)$ and $\mathbf{q}(n; \mathbf{a})$ are the sampled output time histories and the model output vector, respectively; S_o is a selection matrix for the observed DOF. The value $\hat{\sigma}^2(\mathbf{a})$ represents the optimal variance in the prediction error model for given structural model parameters $\mathbf{a}$. Note that for a large number of observed data points N, which is usually the case in practice, the exponent N_J in Equation (1) is a large number and, therefore, the relative posterior probabilities of the various structural model parameters $\mathbf{a}$ are very sensitive to the corresponding values $J(\mathbf{a})$. Specifically, $p(\mathbf{a} \mid \mathscr{D}_N, \mathscr{M}_P)$ becomes negligible everywhere, except for the region of the parameter space where the corresponding values of $J(\mathbf{a})$ are very close to the global minimum $\hat{\sigma}^2 = \min\{J(\mathbf{a}), \mathbf{a} \in S(\mathbf{a})\}$. Thus, the region of important probabilities extends around the points which globally minimize $J(\mathbf{a})$. The parameter values at which $J(\mathbf{a})$ reaches its global minimum are referred to as *optimal* parameters. Note that the model output $\mathbf{q}(n; \mathbf{a})$ involved in the definition of $J(\mathbf{a})$ in Equation (2) is a non-linear function of the parameters $\mathbf{a}$, even in the case of linear dynamic models. Therefore, multiple optimal parameter values may exist for which $J(\mathbf{a})$ might attain its global minimum. This raises the issue of (system) identifiability [2] of these parameters. It is reminded that Reference [2] defines a parameter to be (system) identifiable when there exists either only one optimal value for this parameter (global identifiability) or, in the case where more than one optimal values exist, when the distance between any two optimal values is finite (local identifiability). In a (system) identifiable case the set of optimal parameter points is discrete. Furthermore, assuming that the parameter domain $S(\mathbf{a})$ is bounded, identifiability implies the existence of a finite number of optimal points $\hat{\mathbf{a}}^{(k)}$, $k = 1, \ldots, K$, satisfying

$$J(\hat{\mathbf{a}}^{(k)}) = \min_{\mathbf{a} \in S(\mathbf{a})} J(\mathbf{a}) = \hat{\sigma}^2 \tag{3}$$

where $\hat{\sigma}^2$ represents the overall optimal variance for the prediction error. The task of finding all global minima of the nonconvex function $J(\mathbf{a})$ is non-trivial. Katafygiotis and Beck [3] presented an algorithm to resolve locally identifiable cases. Assuming one optimal value to be known, this algorithm searches efficiently the parameter space to find all other (if any) optimal parameter values corresponding to output-equivalent models.

The optimal prediction-error parameter $\hat{\sigma}$ is always globally identifiable [2] and is given by Equation (3). Therefore, the issue of identifiability concerns only the structural model parameters $\mathbf{a}$. These parameters could be either (globally or locally) identifiable or unidentifiable. The larger the dimension N_a of the parameter vector $\mathbf{a}$, the more likely it is to encounter unidentifiability of $\mathbf{a}$.

Beck and Katafygiotis [2] derived an asymptotic approximation for the posterior PDF of the structural model parameters $\mathbf{a}$ which is valid for identifiable cases and for a large number

N of sampling points:

$$p(\mathbf{a} \mid \mathscr{D}_N, \mathscr{M}_P) \approx \sum_{k=1}^{K} w_k N(\hat{\mathbf{a}}^{(k)}, A_N^{-1}(\hat{\mathbf{a}}^{(k)})) \tag{4}$$

where $N(\boldsymbol{\mu}, \Sigma)$, denotes a multivariate Gaussian distribution with mean $\boldsymbol{\mu}$ and covariance matrix Σ. Equation (4) approximates the posterior PDF of the parameters $\mathbf{a}$ with a finite weighted sum of Gaussian distributions centered at the optimal values $\hat{\mathbf{a}}^{(k)}$, $k = 1, \ldots, K$. The matrix $A_N(\hat{\mathbf{a}}^{(k)})$ in Equation (4) can be shown [2] to be equal to the Hessian of the function $g(\mathbf{a}) = N_J \ln J(\mathbf{a})$ evaluated at $\hat{\mathbf{a}}^{(k)}$. Finally the weighting coefficients w_k are given [2] by

$$w_k = \frac{w_k'}{\sum_{k=1}^{K} w_k'} \quad \text{where } w_k' = \pi(\hat{\mathbf{a}}^{(k)}) |A_N(\hat{\mathbf{a}}^{(k)})|^{-1/2} \tag{5}$$

and account for the total probability in the neighbourhood of each optimal point.

2.2. *Identifiability of order R*

The asymptotic result (4) assumes that the posterior PDF of the parameters is concentrated in the close neighbourhood of a finite number of optimal points. This result is valid only under the following two conditions: (i) the structural model parameter vector $\mathbf{a}$ is (system) identifiable under $\mathscr{D}_N$ and (ii) the number of measured data N is sufficiently large. The reasons for which these two conditions are necessary are as follows. The first condition, namely that of identifiability of $\mathbf{a}$, is required by Equation (4) because it ensures that the set of optimal parameters consists of discrete points. Furthermore, assuming that the parameter domain $S(\mathbf{a})$ is bounded, system identifiability implies the existence of a finite number of optimal points. On the contrary, according to Reference [2] in an unidentifiable case there exists an infinite number of optimal points and the set of these points is not discrete but continuous. A simple example of such an unidentifiable case is that of a SDOF oscillator subjected to ground motion when both the mass and stiffness are included in the parameters to be updated. It is easy to verify in this case that, given an optimal model, all other models with proportional mass and stiffness are output-equivalent and, therefore, also optimal. In this case the set of optimal points corresponds to a straight line in the parameter space and the posterior PDF of the parameters is concentrated in the neighbourhood of this line rather than being concentrated in the neighbourhood of a discrete set of points as assumed in the aforementioned approximation (4). In the general unidentifiable case the set of optimal points forms a manifold $\mathfrak{S} \subset S(\mathbf{a})$ with dimension $1 \leqslant N_{\mathfrak{S}} \leqslant N_a$. In the above SDOF example $N_{\mathfrak{S}} = 1$.

The second condition for validity of Equation (4) is having a sufficiently large number of data N, or equivalently a sufficiently large exponent N_J in Equation (1). This is needed in order to guarantee that $p(\mathbf{a} \mid \mathscr{D}_N, \mathscr{M}_P)$ decays rapidly in all directions around any optimal point. In an identifiable case, this condition ensures that the posterior PDF is concentrated in a number of disjoint regions, each corresponding to the close neighbourhood of an optimal point. If the decay of $p(\mathbf{a} \mid \mathscr{D}_N, \mathscr{M}_P)$ is not sufficiently rapid, the neighbourhoods of significant probability corresponding to different optimal points may be overlapping. In addition, rapid decay of $p(\mathbf{a} \mid \mathscr{D}_N, \mathscr{M}_P)$ ensures that the assumed Gaussian approximation is sufficiently accurate in the neighbourhood of each optimal point where probabilities are significant. Slow decay in certain directions implies that the PDF is concentrated in the close neighbourhood of

a manifold in the parameter space, denoted as earlier by $\mathfrak{S}$, extending along the directions of slow decay. The dimension of the manifold $N_{\mathfrak{S}}$, where $1 \leqslant N_{\mathfrak{S}} \leqslant N_a$, is equal to the number of directions of slow decay. The points on this manifold, other than the optimal points, have corresponding values of $J(\mathbf{a})$ slightly larger than the global minimum value $\hat{\sigma}^2$ and, therefore, have significant probability without necessarily belonging in the close neighbourhood of an optimal point. In this case the finite number of optimal points does not suffice to describe the posterior PDFs of the parameters and the predictive response. This case, although being classified as identifiable according to the definitions in Reference [2], appears to have many similarities to an unidentifiable case, and from a practical standpoint is better classified as 'almost' unidentifiable with the points on the manifold behaving as 'almost' optimal points.

The above discussion leads to a new stricter definition for identifiability, to which we will refer to as *system identifiability of order R*, where $R \geqslant 0$.

Definition. The model parameters $\mathbf{a}$ are said to be *system identifiable of order* $R \geqslant 0$ for the class $\mathscr{M}_P$ and for given data $\mathscr{D}_N$ if for any optimal parameter $\hat{\mathbf{a}}$, i.e. for any value $\hat{\mathbf{a}}$ such that: $J(\hat{\mathbf{a}}) = \min_{\mathbf{a} \in S(\mathbf{a})} J(\mathbf{a})$, the following condition is satisfied:

$$\min_{1 \leqslant i \leqslant N_a} \lambda_i(A_N(\hat{\mathbf{a}})) > R \geqslant 0 \tag{6}$$

where $A_N(\hat{\mathbf{a}})$ is the matrix appearing in Equation (4), namely the Hessian matrix of the function $g(\mathbf{a}) = N_J \ln J(\mathbf{a})$ evaluated at $\hat{\mathbf{a}}$, and $\lambda_i(A_N(\hat{\mathbf{a}}))$, $i = 1, \ldots, N_a$ are the eigenvalues of this matrix.

The above definition ensures that the set of optimal points is discrete because it requires the Hessian of $J(\mathbf{a})$ to be a positive definite matrix as can be seen from definition (6). Furthermore, assuming a slowly varying prior distribution, it ensures that the curvature of the function $-\ln p(\mathbf{a} \mid \mathscr{D}_N, \mathscr{M}_P)$ calculated in any direction and at any of the optimal points is larger than $R \geqslant 0$. This guarantees that if one moves away from any optimal point by a distance x in any direction, the PDF will decay faster than $\exp(-Rx^2/2)$. Let us introduce a threshold value ε, where $0 < \varepsilon < 1$, such that only points with normalized (with respect to the global maximum) PDF values larger than ε be considered as having significant probability. An alternative definition for identifiability (involving two parameters r and ε) is: 'The parameter vector $\mathbf{a}$ is said to be identifiable if the neighbourhood of significant probabilities (specified by ε) around any optimal point $\hat{\mathbf{a}}$ is contained within a sphere of radius r centered at $\hat{\mathbf{a}}$'. The latter definition seems more natural but involves the specification of two parameters. By choosing R so that $\varepsilon = \exp(-Rr^2/2)$ the two definitions become equivalent. The latter observation is useful for selecting the desired value for the parameter R. Clearly, the larger R the stricter the definition of identifiability becomes. It must be noted that system identifiability of the parameters $\mathbf{a}$ according to the definition in Reference [2] corresponds to system identifiability of order $R = 0$ under the new definition.

2.3. Unidentifiable cases

Based on this new definition, unidentifiability receives a less restrictive interpretation. The strict definition of unidentifiability in Reference [2] corresponds to the particular case of

unidentifiability of order $R=0$. In this case at least one of the eigenvalues $\lambda_i(A_N(\hat{\mathbf{a}}))$ is zero. Therefore, there exist one or more directions along which $J(\mathbf{a})$ remains perfectly flat as one moves away from an optimal point, which implies the existence of a non-discrete (infinite) set of optimal solutions. Unidentifiability of order $R>0$ means that there exists a non-empty set of eigenvalues being less or equal to R. This implies either a non-discrete (infinite) set of optimal solutions (when one or more of these eigenvalues are equal to zero), or a finite number of optimal solutions but with unsatisfactory decay rate. In an unidentifiable case of order R, the region of significant probabilities is contained in the neighbourhood of a manifold $\mathfrak{S}$, with dimension $N_{\mathfrak{S}}$ determined by the number of the eigenvalues $\lambda_i(A_N(\hat{\mathbf{a}}))$ which satisfy the condition $\lambda_i(A_N(\hat{\mathbf{a}}))\leqslant R$. Here, the region of significant probabilities and the neighbourhood of the manifold are assumed to be specified as earlier through the parameters ε and r, respectively. Thus, the region of significant probability refers to points with normalized PDF values larger than ε, and the neighbourhood of the manifold refers to the points of the parameter space which lie at distance less or equal to r from some point on the manifold, where $\varepsilon=\exp(-Rr^2/2)$. Clearly in an unidentifiable case $1\leqslant N_{\mathfrak{S}}\leqslant N_a$. Note that the parameter ε, used to specify the region of points with significant probability, can be also used to define the boundaries of $\mathfrak{S}$. That is, $\mathfrak{S}$ extends around the optimal points in the directions along which $J(\mathbf{a})$ is flat or almost flat and until the value of $J(\mathbf{a})$ reduces to the level where the corresponding normalized probabilities become less than ε. Finally, note that $\mathfrak{S}$ may be disconnected, that is, it may consist of several disjoint regions each containing one or more optimal points.

One can extend the concept of the manifold to identifiable cases by considering in this case the manifold to be the discrete set of optimal points. Clearly, in this degenerate case the dimension of the manifold is $N_{\mathfrak{S}}=0$. Based on this generalized interpretation of the manifold $\mathfrak{S}$, one can state that always, in both identifiable and unidentifiable cases, the posterior PDF of the parameters is concentrated in the neighbourhood of the manifold $\mathfrak{S}$. Note that here, and throughout the remaining of this paper unless explicitly otherwise mentioned, the terms identifiability and unidentifiability are used in the context of the new definition introduced above, that is, assuming a chosen value for R.

It follows from the above discussion that the distinctive difference between identifiable and unidentifiable cases lies in the dimension of the corresponding manifold. In an identifiable case the manifold $\mathfrak{S}$ has dimension zero and can be expressed as the finite set of optimal values $\mathfrak{S}=\{\hat{\mathbf{a}}^{(k)},\ k=1,\ldots,K\}$. This allows for the model updating problem to be reduced to finding the finite number of optimal points comprising $\mathfrak{S}$. References [2, 5] provide the tools to resolve this problem. On the other hand, in the unidentifiable case the dimension of the manifold $\mathfrak{S}$ is $N_{\mathfrak{S}}\geqslant 1$; this makes the model updating problem much more complicated since all the points on the manifold, an infinite non-discrete set of points in this case, have significant probabilities and should be accounted for when attempting an approximate representation of the posterior PDF of the parameters.

2.4. *Treatment of unidentifiable cases*

In the absence of any analytical solutions, the calculation and meaningful representation of $\mathfrak{S}$ can be achieved by generating a finite set of points $A=\{\mathbf{a}^{(l)},\ l=1,\ldots,L\}$ on the manifold. The posterior PDF of the uncertain model parameters can then be approximated by a weighted

sum of Dirac delta functions centered at these points [6] as follows:

$$p(\mathbf{a} \mid \mathscr{D}_N, \mathscr{M}_P) \approx \sum_{l=1}^{L} w_l \delta(\mathbf{a} - \mathbf{a}^{(l)}) \tag{7}$$

where the weightings w_l represent the relative volume of the PDF in the neighbourhood of each point $\mathbf{a}^{(l)}$. Using the theorem of total probability, the posterior predictive response can be approximated by the weighted sum of the predictive responses of the models with parameters in the set A, using the same weightings w_l. It was shown in Reference [6] that the coefficients w_l are given by

$$w_l = c_2 J(\mathbf{a}^{(l)})^{-N_J} \pi(\mathbf{a}^{(l)}) |B_N(\mathbf{a}^{(l)})|^{-1/2} I(\mathbf{a}^{(l)}) \tag{8}$$

where c_2 is a normalizing constant such that the sum of all w_l's is equal to unity. The next four factors in the right-hand side of Equation (8) are in the order they appear proportional to: (i) the relative value of the posterior PDF at point $\mathbf{a}^{(l)}$, assuming non-informative (uniform) prior, (ii) the value of the prior PDF at point $\mathbf{a}^{(l)}$, (iii) the *thickness* of the manifold, expressed as the relative volume of the PDF in the neighbourhood of $\mathbf{a}^{(l)}$ in the space perpendicular to the manifold, and (iv) a *spacing* factor which reflects the relative tributary area of the manifold corresponding to the point $\mathbf{a}^{(l)}$. The matrix $B_N(\mathbf{a}^{(l)})$ appearing in the thickness factor denotes the restriction of $A_N(\mathbf{a}^{(l)})$ in the $(N_a - N_{\mathfrak{S}})$-dimensional subspace which is perpendicular to the manifold $\mathfrak{S}$ at the point $\mathbf{a}^{(l)}$. It can be shown that the thickness weighting factor can be calculated according to

$$\left|B_N(\mathbf{a}^{(l)})\right|^{-1/2} = \prod_{i=N_{\mathfrak{S}}+1}^{N_a} \lambda_i^{(l)^{-1/2}} \tag{9}$$

where $\lambda_i^{(l)}$, $l = 1, \ldots, N_a$, are the eigenvalues of $A_N(\mathbf{a}^{(l)})$ assumed in an ascending order. Thus, the thickness weighting factor is equal to the inverse square root of the product of all eigenvalues of $A_N(\mathbf{a}^{(l)})$ that are larger than R.

The spacing factor $I(\mathbf{a}^{(l)})$ accounts for the non-uniform distribution of the points $\mathbf{a}^{(l)}$ on the manifold. In the case of a one-dimensional manifold the spacing factor can be easily established as being proportional to the average distance between the point $\mathbf{a}^{(l)}$ and its two immediate neighbouring points (one on each side). However, as one moves to manifolds of dimension two or higher, one faces a difficulty in defining the concept of neighbouring points and in assigning an algorithm for calculating the spacing coefficient.

In Reference [6] an algorithm was presented for the calculation of a representative set of points A. This algorithm was based on a series of constrained minimizations over a grid of N_a-dimensional cubes which is self-expanding along the directions of the manifold. The adaptive expansion of this grid allows for only a small region of the total parameter space containing the manifold to be explored, thus making it computationally efficient. One of the difficulties encountered by that algorithm is in the calculation of the weighting coefficients w_l corresponding to the various points $\mathbf{a}^{(l)} \in A$. In particular, this algorithm generates a grid of points which are not uniformly distributed and faces the aforementioned difficulty of calculating the spacing coefficient $I(\mathbf{a}^{(l)})$ when dealing with manifolds of dimension $N_{\mathfrak{S}} > 1$. This difficulty severely limits the applicability of the algorithm to the case of one-dimension manifolds ($N_{\mathfrak{S}} = 1$). Furthermore, the efficiency of the algorithm is not fully optimized as the search for points on the manifold is performed in all directions. That is, the algorithm does

not take full advantage of the knowledge that the dimension of the manifold is usually much smaller than the dimension of the parameter space in which it lies.

3. TANGENTIAL-PROJECTION (TP) ALGORITHM FOR MANIFOLD REPRESENTATION

Herein we present a new algorithm for generating a representative set of points A for the manifold. The proposed algorithm builds the set A in an adaptive expansive manner. The points in A are calculated as being the projections on the manifold of appropriately generated grid points lying in different tangential subspaces of the manifold. Therefore, this algorithm is referred to as the tangential-projection (TP) algorithm. The TP algorithm has the following properties: (i) it is computationally more efficient than the algorithm in Reference [6], (ii) it produces a more uniform grid of points, (iii) it allows for a straightforward computation of the weightings w_l, and (iv) it can be easily generalized to manifolds of any dimension. The algorithm has a structured methodology for determining an appropriate unique set of immediate neighbours for each point $\mathbf{a}^{(l)}$. Once this set of neighbours is determined one can easily proceed with the calculation of the corresponding tributary area and the corresponding spacing coefficient.

Next, we present an overview of the steps of the TP algorithm for calculating the representative set A. The algorithm assumes that a selection of some controlling parameter values is made at the beginning. In particular, one must select the value of the parameter ε specifying the threshold of significant probabilities, a value R for the desired order of identifiability, and a value for a parameter Δr which determines the approximate distance between neighbouring points in the generated set A. The value of Δr is usually selected to be of the order of the maximum 'thickness' r of the manifold which is determined as $r=(-2\log(\varepsilon)/R)^{1/2}$.

The first point $\mathbf{a}^{(1)}\in A$ is calculated using an unconstrained minimization of the function $J(\mathbf{a})$. Once $\mathbf{a}^{(1)}$ is found, the dimension $N_{\mathfrak{S}}$ of the manifold $\mathfrak{S}$ is established by solving the eigenvalue problem for $A_N(\mathbf{a}^{(l)})=\nabla^2 g(\mathbf{a}^{(1)})$; $N_{\mathfrak{S}}$ is equal to the number of eigenvalues which are smaller or equal to R; the eigenvectors corresponding to these eigenvalues span a subspace tangential to the manifold at the point $\mathbf{a}^{(1)}$.

In the following discussion we will assume for simplicity that $N_{\mathfrak{S}}=2$. This relatively simple case is selected here because it allows for a clear geometric interpretation of the steps involved, especially if one considers a parameter space of dimension $N_a=3$; in this case one can visualize the manifold as a two-dimensional surface in the three-dimensional parameter space. We did not choose to present the even simpler case $N_{\mathfrak{S}}=1$ because in that case some of the fundamental difficulties faced in higher-dimensional cases are not raised; for example, in the case of a one-dimensional manifold it is straightforward to define the neighbours of any point $\mathbf{a}^{(l)}$ as the points to the left and right of $\mathbf{a}^{(l)}$, but the extension of this neighbouring concept in higher dimensions is not trivial. We have chosen to present the case $N_{\mathfrak{S}}=2$ because it is relatively simple to illustrate and at the same time it can be extended to higher-dimensional cases without too much difficulty.

One of the basic ideas of the TP algorithm is to generate the points $\mathbf{a}^{(l)}\in A$ in a specific strictly structured manner. Two fundamental concepts are used towards this end: the first concept is that of parent–child point relationship, and the second is that of neighbouring points. These concepts are discussed in detail next in Sections 3.1 and 3.2, respectively. In Section 3.3 these concepts are illustrated with an example.

3.1. Parent–child point relationship

The TP algorithm consists of a series of point generation (or point expansion) steps. During the lth step, points are generated around point $\mathbf{a}^{(l)}$; the points generated during this step are referred to as the child-points of $\mathbf{a}^{(l)}$, while $\mathbf{a}^{(l)}$ is referred to as the parent-point of the newly generated points. Thus, for each point $\mathbf{a}^{(l)}$, except for point $\mathbf{a}^{(1)}$, there exists a unique parent-point which has generated it. Therefore, one can define a 'parent' function $\mathscr{P}$ mapping the set $\{2,\ldots,L\}$ within the set $\{1,\ldots,L-1\}$ in such a way that the relationship '$\mathbf{a}^{(l)}$ is parent of $\mathbf{a}^{(s)}$' can be mathematically expressed as $\mathscr{P}(s)=l$. Note the fact that this mapping is within, and generally not on, the set $\{1,\ldots,L-1\}$ which implies that there may exist points in the set $\{2,\ldots,L-1\}$ which are not parents of any point. Furthermore, the function $\mathscr{P}$ is not invertible, implying that some point may be the parent of several different points. Although we cannot define $\mathscr{P}^{-1}$ as a function, we can define it as an inverse image, that is, for $l\in\{1,\ldots,L-1\}$, we define the set $\mathscr{P}^{-1}(\{l\})$ as follows:

$$\begin{aligned}\mathscr{P}^{-1}(\{l\}) &= \{s:\ 2\leqslant s\leqslant L;\mathscr{P}(s)=l\}\\ &= \{s_{l1},s_{l2},\ldots,s_{ln_l}\}\end{aligned} \tag{10}$$

where n_l is the total number of child-points corresponding to point $\mathbf{a}^{(l)}$. Thus, $\mathscr{P}^{-1}(\{l\})$ defines the set of all child points for point $\mathbf{a}^{(l)}$. If point $\mathbf{a}^{(l)}$ does not generate any points then $\mathscr{P}^{-1}(\{l\})$ is an empty set. In our particular algorithm, as will be seen later in this section, each point may be the parent of zero up to $2\times N_{\mathfrak{S}}=4$ child-points, that is, $0\leqslant n_l\leqslant 4$. The order of generation of points is reflected by their numbering; for example, point $\mathbf{a}^{(l)}$ is the lth generated point in the set A. Therefore, it follows that $\mathscr{P}(l)<l$, for any point $l\in\{2,\ldots,L\}$.

There are a few rules mandating the order of point generation:

1. The first rule is that a point $\mathbf{a}^{(l)}$ can become a parent if and only if it has a corresponding relative PDF value (with respect to the largest value encountered so far) larger than the threshold value ε. This rule ensures that the expansion of the manifold does not continue beyond points with relatively insignificant probability values. In particular, a point $\mathbf{a}^{(l)}$ with relative PDF value less than ε, lies just outside the boundary of the manifold; such points are hereafter referred to as 'boundary' points, or 'inactive' points because they do not generate child points. On the contrary, points with relative PDF value larger than ε, belong to the interior of the manifold and are hereafter referred to as 'interior' or 'active' points.
2. The second rule is that the lth point, assuming it is active, may become a parent only after all other active points $\mathbf{a}^{(k)}$, with $k<l$, have generated all their child-points. A corollary of this rule is that all child-points generated by a single parent-point are numbered consecutively.
3. The last rule refers to the calculation and the numbering of the child-points generated by a specific (active) parent-point $\mathbf{a}^{(l)}$. This is described in detail in the following subsection.

3.1.1. Generation of child points of $\mathbf{a}^{(l)}$. Let $\lambda_1^{(l)}$ and $\lambda_2^{(l)}$ denote the lowest two eigenvalues of $\nabla^2 g(\mathbf{a}^{(l)})$, assumed in ascending order, and let $\boldsymbol{\psi}^{(l),1}$ and $\boldsymbol{\psi}^{(l),2}$, respectively, denote the corresponding eigenvectors, normalized so that their length is equal to one. In order to

uniquely specify these vectors, that is, in order to uniquely select one out of the two possible (opposite to one another) solutions, an additional condition is imposed: the inner products $\langle \boldsymbol{\psi}^{(l),i}, \boldsymbol{\psi}^{(s),i} \rangle$, $i = 1, 2$, $s = \mathscr{P}(l)$, are required to be positive. Note that the choice of positive direction for the eigenvectors $\boldsymbol{\psi}^{(1),1}, \boldsymbol{\psi}^{(1),2}$ corresponding to point $\mathbf{a}^{(1)}$ is arbitrary, but once selected, it determines the positive direction of the eigenvectors of all follow-up generated points. Clearly the eigenvectors $\boldsymbol{\psi}^{(l),1}, \boldsymbol{\psi}^{(l),2}$ span a plane tangential to the manifold at point $\mathbf{a}^{(l)}$. Using these eigenvectors, an ordered set $B^{(l)}$ is generated, comprised of four points within the aforementioned tangential plane, as follows:

$$B^{(l)} = \{\mathbf{a}^{(l)} - \Delta r \boldsymbol{\psi}^{(l),1}, \mathbf{a}^{(l)} + \Delta r \boldsymbol{\psi}^{(l),1}, \mathbf{a}^{(l)} - \Delta r \boldsymbol{\psi}^{(l),2}, \mathbf{a}^{(l)} + \Delta r \boldsymbol{\psi}^{(l),2}\} \tag{11}$$

Once the set $B^{(l)}$ is determined, then the final step of the child-point generation process for $\mathbf{a}^{(l)}$ can be performed. Starting from each point $\mathbf{b}^{(l),i} \in B^{(l)}$, $i = 1, \ldots, 4$ (in the given order), and under some conditions based on the concept of neighbouring points discussed later in Section 3.2.2, minimization of $J(\mathbf{a})$ is performed within the $(N_a - 2)$-dimensional subspace which contains $\mathbf{b}^{(l),i}$ and is orthogonal to $\boldsymbol{\psi}^{(l),1}$ and $\boldsymbol{\psi}^{(l),2}$; this is achieved by performing a minimization in the space spanned by the eigenvectors $\boldsymbol{\psi}^{(l),i}$, $i = 3, \ldots, N_a$. The point at which the minimum is reached corresponds to a new child-point for $\mathbf{a}^{(l)}$ and is assigned the next available point ordering number. Obviously, the maximum number of child-points generated by this process is four, and this happens if all points $\mathbf{b}^{(l),i}$, $i = 1, \ldots, 4$, satisfy the neighbourhood conditions discussed later in Section 3.2.2.

3.2. Neighbouring point relationship

Here we discuss the second fundamental concept of the proposed algorithm, namely the concept of neighbouring points. This relationship is the controlling factor for deciding whether or not to perform the minimization step starting from point $\mathbf{b}^{(l),i}$ described in the previous section.

According to the neighbouring concept, each point $\mathbf{a}^{(l)} \in A$ may have a maximum of $2 \times N_{\mathfrak{S}} = 4$ neighbouring points in A; if $\mathbf{a}^{(l)}$ is an interior (active) point of the manifold then the number of neighbouring points is equal to four, while if it is a boundary (inactive) point then this number is less than four. Each of the neighbouring points of $\mathbf{a}^{(l)}$ is located on the manifold in approximately one of the following four directions relative to $\mathbf{a}^{(l)}$: the negative or positive major direction (specified by $\boldsymbol{\psi}^{(l),1}$) or the negative or positive minor direction of the manifold (specified by $\boldsymbol{\psi}^{(l),2}$). To each point $\mathbf{a}^{(l)}$ we assign a uniquely determined ordered set $C^{(l)}$ with four elements containing all its neighbouring points. The ordering of these points in the set $C^{(l)}$ is chosen to follow a similar convention as the one adopted for the set $B^{(l)}$ in Equation (11). For example, the first point in the set $C^{(l)}$ is the neighbouring point located approximately along the negative major direction of the manifold relative to $\mathbf{a}^{(l)}$; if there is no such point (as may happen if $\mathbf{a}^{(l)}$ lies on the manifold boundary) then the first position in the set $C^{(l)}$ is left empty.

The set $C^{(l)}$ plays a significant role in the proposed algorithm because of the following two reasons: (i) it is used to determine the spacing weighting factor $I(\mathbf{a}^{(l)})$ in Equation (8); this factor is taken to be equal to the total area enclosed by the set of the neighbouring points of $\mathbf{a}^{(l)}$; and (ii) it is used to determine which particular elements of the aforementioned set $B^{(l)}$ can lead to the generation of new child-points; thus, $C^{(l)}$ directly controls the directions

of point expansion around $\mathbf{a}^{(l)}$ as is explained in further detail in Section 3.2.2. First, in the next section we discuss the rules for establishing $C^{(l)}$.

3.2.1. Continual updating of $C^{(l)}$. An important feature of the proposed algorithm is that the two important functions of point generation and neighbourhood establishment are done in parallel. After the generation of each new point $\mathbf{a}^{(s)}$, and before proceeding with the generation of any next point, the algorithm efficiently updates all sets $C^{(l)}$, $l<s$, being affected by the generation of this new point. Thus, the sets $C^{(l)}$ are kept fully updated at all times so as to fully reflect all neighbouring relationships that can be established up to the given time.

The continual updating of the sets $C^{(l)}$ is based on a few well-defined rules which follow from some basic properties that the neighbouring relationship is required to have. The first property is that of symmetry, which can be stated mathematically as follows:

$$\mathbf{a}^{(l)} \sim \mathbf{a}^{(s)} \;\Leftrightarrow\; \mathbf{a}^{(s)} \sim \mathbf{a}^{(l)} \tag{12}$$

where $\mathbf{a} \sim \mathbf{b}$ denotes that point $\mathbf{a}$ is a neighbour of point $\mathbf{b}$. This property can also be rewritten as

$$l \in C^{(s)} \;\Leftrightarrow\; s \in C^{(l)} \tag{13}$$

Furthermore, knowing the position of l in the ordered set $C^{(s)}$ helps us to uniquely determine the position of s in the set $C^{(l)}$. For example, based on the aforementioned ordering scheme, it easily follows that if l is the first (third) element of $C^{(s)}$ then s will be the third (first) element of $C^{(l)}$.

The second 'neighbouring' property can be written as

$$\mathscr{P}(s) = l \Rightarrow \mathbf{a}^{(l)} \sim \mathbf{a}^{(s)} \tag{14}$$

or equivalently,

$$\mathscr{P}(s) = l \Rightarrow l \in C^{(s)} \quad \text{and} \quad s \in C^{(l)} \tag{15}$$

In Equation (15) the position which l occupies in the ordered set $C^{(s)}$ uniquely determines the position of s in the set $C^{(l)}$. Specifically, depending on whether l occupies the 1st, 2nd, 3rd or 4th position in $C^{(s)}$, l occupies the 2nd, 1st, 4th and 3rd position in $C^{(l)}$, respectively. The above equations state that a parent–child relationship between two points implies that these point are neighbours of one another (while the reverse is obviously not necessarily true). It follows as a corollary that the set $\mathscr{P}^{-1}(\{l\})$ with $l \geqslant 2$ has a maximum of three elements; that is, $\mathbf{a}^{(l)}$, $l \geqslant 2$, generates no more than three child-points. The proof follows easily from the fact that $C^{(l)}$, which contains a total of the most four elements, must definitely contain the ordering members of the parent point and all the child-points of $\mathbf{a}^{(l)}$. The above case of parent–child neighbouring relationship is also referred to as a 'first-generation' neighbouring relationship.

The last property refers to the so-called 'second-generation' neighbouring relationship. It can be shown that in our case this is the only alternative possibility for a neighbouring relationship between two points to exist. Specifically, it can be shown that

$$\mathbf{a}^{(s)} \sim \mathbf{a}^{(l)},\ s > l, \quad \mathscr{P}(s) \neq l \Rightarrow \mathscr{P}(l) = \mathscr{P}^2(s) \tag{16}$$

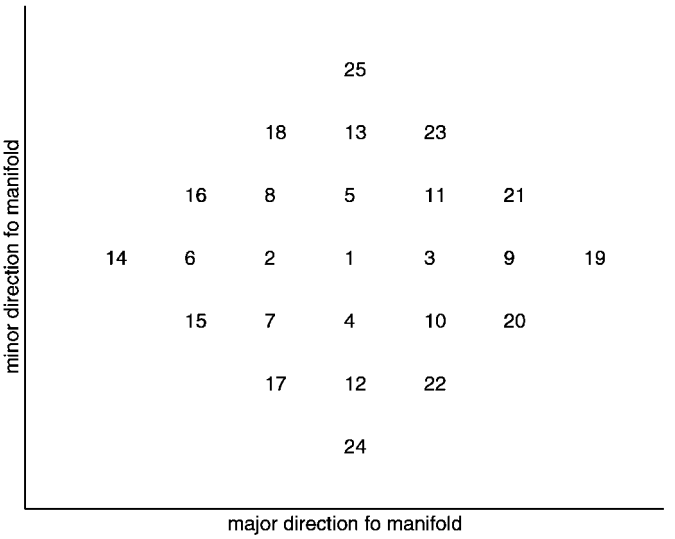

Figure 1. Numbering system for point generation.

where $\mathscr{P}^2(s)=\mathscr{P}(\mathscr{P}(s))$. Equation (16) states that if two points $\mathbf{a}^{(l)}$ and $\mathbf{a}^{(s)}$ with $s>l$ are neighbouring points, without having a first-generation relationship, then the grandparent of (the younger) sth point is the parent of the (older) lth point. However, it must be noted that the condition $\mathscr{P}(l)=\mathscr{P}^2(s)$ does not necessarily imply that $\mathbf{a}^{(s)}\sim\mathbf{a}^{(l)}$. Specifically, it can be shown that a newly generated point $\mathbf{a}^{(s)}$ may have a second-generation relationship only with up to two out of the four points $\mathbf{a}^{(l)}$ satisfying the above condition, i.e. out of the points satisfying $l\in\mathscr{P}^{-1}\{\mathscr{P}^2(s)\}$. An additional set of rules are used to establish such point(s) $\mathbf{a}^{(l)}$ and the position of l and s in the sets $C^{(s)}$ and C^l, respectively. This set of rules are straightforward and are not listed here because of space limitations.

3.2.2. Neighbouring condition for child-generation. The status of the set $C^{(l)}$ at the time of point expansions around $\mathbf{a}^{(l)}$ determines how many and, more specifically, which child points will be generated by $\mathbf{a}^{(l)}$. In particular, the condition for performing a minimization starting from point $\mathbf{b}^{(l),i}\in B^{(l)}$ depends on whether the corresponding ith element of $C^{(l)}$ has already been assigned a value at the time when the point expansion step around $\mathbf{a}^{(l)}$ takes places. If the ith place in the set $C^{(l)}$ is still empty at that time, this implies that no neighbouring point has yet been established in the corresponding direction and thus the minimization step must be performed in order to establish such a neighbouring point. On the contrary, if the ith place in the set $C^{(l)}$ has been assigned an integer value s, this implies that the point $\mathbf{a}^{(s)}$ has already been established as the neighbouring point of $\mathbf{a}^{(l)}$ corresponding to this ith direction and therefore, minimization starting from $\mathbf{b}^{(l),i}$ does not need to be performed.

3.3. Schematic illustration of TP algorithm's concepts

Various points in the earlier sections become clearer with the help of Figure 1 and Table I. Figure 1 illustrates the numbering of the first 25 points of a two-dimensional manifold.

Table I. Sets $C^{(l)}$ after the fifth point-generation step.

		Point												
		1	2	3	4	5	6	7	8	9	10	11	12	13
	$X-$	$2^{(1)}$	$6^{(2)}$	$1^{(1)}$	$7^{(2)}$	$8^{(2)}$				$3^{(3)}$	$4^{(3)}$	$5^{(3)}$		
	$X+$	$3^{(1)}$	$1^{(1)}$	$9^{(3)}$	$10^{(3)}$	$11^{(3)}$	$2^{(2)}$	$4^{(2)}$	$5^{(2)}$					
$C^{(l)}$	$Y-$	$4^{(1)}$	$7^{(2)}$	$10^{(3)}$	$12^{(4)}$	$1^{(1)}$			$2^{(2)}$			$3^{(3)}$		$5^{(5)}$
	$Y+$	$5^{(1)}$	$8^{(2)}$	$11^{(3)}$	$1^{(1)}$	$13^{(5)}$		$2^{(2)}$			$3^{(3)}$		$4^{(4)}$	

Here, x and y correspond to the major and minor direction of the manifold. Table I depicts the updated neighbouring sets $C^{(l)}$ right after the fifth point-generation step, i.e. right after all child-points of point 5 have been generated. The numbers in the superscript denote the point-generation step during which a particular point was generated and during which the neighbouring sets were updated.

Starting with point 1, during the first point-generation step points 2, 3, 4 and 5 are generated sequentially to the left, right, bottom and top of point 1, respectively. Points 2, 3, 4 and 5 are the child points of point 1, i.e. $\mathscr{P}^{-1}(1)=\{2,3,4,5\}$. At the end of this first step the updated neighbouring sets are as follows: $C^{(1)}=\{2,3,4,5\}$, $C^{(2)}=\{,1,,\}$, $C^{(3)}=\{1,,,\}$, $C^{(4)}=\{,,,1\}$ and $C^{(5)}=\{,,1,\}$. During the second point-generation step point 2 generates three child points: 6 to its left, 7 to its bottom and 8 to its top (see Figure 1). Note that no point is generated to its right as the set $C^{(2)}$ had already its second position filled by the number 1, implying that the right neighbour of $\mathbf{a}^{(2)}$ already exists and is point $\mathbf{a}^{(1)}$. At the end of this second step the updated neighbouring sets are $C^{(1)}=\{2,3,4,5\}$, $C^{(2)}=\{6,1,7,8\}$, $C^{(3)}=\{1,,,,\}$, $C^{(4)}=\{7,,,1\}$, $C^{(5)}=\{8,,1,\}$, $C^{(6)}=\{,2,,\}$, $C^{(7)}=\{,4,,2\}$ and $C^{(8)}=\{,5,2,\}$. Notice that the relationships between points 7 and 4 and between 5 and 8 are second-generation ones. During the third point-generation step, point 3 generates points 9, 10 and 11. Again, notice that no point is generated to the left of point 3 as the first space in the set $C^{(3)}$ is already occupied by point 1. Again, the neighbouring sets are updated appropriately. For example, after this third point-generation step $C^{(4)}=\{7,10,,1\}$. Note that the relationships between points 4 and 7 and 4 and 10 are both second-generation ones. As $C^{(4)}$ has only one empty space at the third position, during the next (fourth) point-generation step only point 12 is generated at the bottom of point 4. The procedure continues in a similar manner as shown in Figure 1 and Table I.

3.4. Overview of tangential-projection algorithm

Having described the basic properties of the point generating process and of the process for continual updating of the neighbouring relationships, the proposed algorithm can be summarized as follows:

The algorithm consists of a set of point-generation steps. During the lth point-generation step the algorithm does the following:

1. It checks whether point $\mathbf{a}^{(l)}$ is an interior (active) or a boundary (inactive) point. If it is a boundary point, the algorithm skips the next two steps and returns to this step

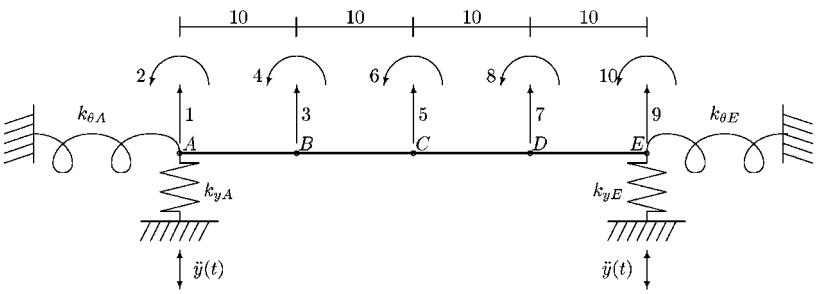

Figure 2. Bridge model.

for the next $(l+1)$th point-generation step. Otherwise, the following steps 2 and 3 are performed.

2. It solves the eigenvalue problem of $\nabla^2 g(\mathbf{a}^{(l)})$ and establishes the set $B^{(l)}$ according to Equation (11). Next, it performs the appropriate (N_a-2)-dimensional minimizations starting at the eligible (based on the current state of the set $C^{(l)}$) points of $B^{(l)}$ to obtain sequentially the child-points of $\mathbf{a}^{(l)}$.
3. For each generated child-point all possible new first- and second-generation neighbourhood relationships are established and the corresponding sets $C^{(l)}$ for all affected points are updated.

The algorithm continues until all point expansions have reached the manifold boundary and there are no more active points to be considered. In order to account for the possibility of the manifold being disconnected, the algorithm does not stop when the above described process finishes. Instead, the point with maximum probability is identified from the current set of points, and using the algorithm presented in Reference [3] all output-equivalent points in the parameter space are located. For each such output-equivalent point we check whether or not it belongs in the region of the parameter space already explored and having yielded the current set of points A. If it does not belong in this region, then the algorithm presented in this section is repeated with this new point as starting point $\mathbf{a}^{(1)}$. This procedure allows for the representation of the manifold by a finite set of points, even when the manifold is disconnected.

Once the final set of points A is established, the corresponding weighting weightings w_l can be calculated according to Equation (8). The spacing coefficient $I(\mathbf{a}^{(l)})$ is chosen to be proportional to the total area enclosed by the set of neighbouring points of $\mathbf{a}^{(l)}$.

4. NUMERICAL EXAMPLE

The proposed methodology is demonstrated using a numerical example involving a two-dimensional 10-DOF finite element model of a single-span elastically supported bridge as shown in Figure 2. The bridge is assumed to be subjected to a ground motion given by the NS 1940 El Centro earthquake record. Only one DOF, the translational DOF at the midspan C, is assumed to be measured.

Table II. Representation of different uncertain parameters for models M1 and M2.

Model	Translational spring		Rotational spring		Bending rigidity
	Node A	Node E	Node A	Node E	
M1	$\theta_1 k_{yA}$	$\theta_2 k_{yE}$	$\theta_3 k_{\theta A}$	$\theta_3 k_{\theta E}$	$\theta_4 EI$
M2	$\theta_1 k_{yA}$	$\theta_3 k_{yE}$	$\theta_2 k_{\theta A}$	$\theta_4 k_{\theta E}$	$\theta_5 EI$

The structural parameters for the nominal structure are as follows: translational spring constants $k_{yA} = 1.1 \times 10^7$ N/m and $k_{yE} = 0.9 \times 10^7$ N/m; rotational spring constants $k_{\theta A} = 1.2 \times 10^5$ N m and $k_{\theta E} = 0.85 \times 10^5$ N m; bending rigidities of elements AB, BC, CD and DE equal to $0.95\,EI$, $1.05\,EI$, $0.9\,EI$ and $0.95\,EI$, respectively, where $EI = 10^6$ N m^2; lumped mass at each node equal to $m_A = m_E = 8 \times 10^3$ kg, and $m_B = m_C = m_D = 16 \times 10^3$ kg. The measurement data were simulated by adding a 20 per cent white noise to the calculated response of the nominal structure.

Two models, denoted as M1 and M2, with different degrees of complexity were employed in the model updating process. Both models are based on the same reference model with structural parameters as follows: translational spring constants $k^*_{yA} = k^*_{yE} = 10^7$ N/m; rotational spring constants $k^*_{\theta A} = k^*_{\theta E} = 10^5$ N m; uniform bending rigidity along the bridge desk equal to $EI^* = 10^6$ N m^2. Model M1 involves four stiffness scaling parameters (denoted by θ_i, $i = 1, \ldots, 4$) allowing for an independent scaling of the translational springs at each end, a common scaling of the rotational springs at both ends, and a uniform scaling of the deck rigidity. Model M2 differs from M1 in that it allows for an independent scaling of the rotational springs at each end, thus involving a total of five stiffness scaling parameters (denoted by θ_i, $i = 1, \ldots, 5$). Table II lists the stiffness characteristics of the two models M1 and M2, as a function of the corresponding θs. Twenty seconds of data with a sampling interval of $\Delta t = 0.02$ were used, i.e. $N = 1000$ points were used in the model updating.

Based on the proposed algorithm, the manifolds for both models are generated. Owing to the different degree of complexity of the two models, the manifold for M1 is found to be one-dimensional (circles in Figure 3(a)–3(c)) while that for M2 is found to be two-dimensional (dots in Figure 3(a)–3(c)). Figure 3(a)–3(c) depict the manifolds plotted in three different subspaces of the parameter space, referred to as subspace A, B and C. Subspace A is the subspace $(\theta_1, \theta_3, \theta_4)$ and $(\theta_1, \theta_2, \theta_5)$ for M1 and M2, respectively. Subspace B is the subspace $(\theta_3, \theta_3, \theta_4)$ and $(\theta_2, \theta_4, \theta_5)$ for M1 and M2, respectively. Subspace C is the subspace $(\theta_1, \theta_2, \theta_4)$ and $(\theta_1, \theta_3, \theta_5)$ for M1 and M2, respectively. As can be seen from these figures, the one-dimensional manifold of M1 is a subset of the two-dimensional manifold of M2.

It is evident from Figure 3(a) that both the above one-dimensional and the two-dimensional manifolds are disconnected. Therefore, in both cases, initially only one part of the manifold was calculated using the above algorithm. Then, starting from the point with the largest probability, and using the algorithm presented in Reference [3], we were able to find another output-equivalent point, having equally large probability and not belonging in the already identified part of the manifold. Restarting from this new point the TP algorithm we were able to construct the second part of the manifold. It can be seen that the two disconnected manifold parts exhibit some symmetry as expected. For example, interchanging the values of θ_1 and θ_2 for a point on one part of the manifold of M1 leads to a point on the second

part of the manifold. Similarly in M2 one may interchange the values of the sets (θ_1, θ_2) and (θ_3, θ_4) to obtain a point on the other part of the manifold. A study of the effect of different sensor locations on the calculated manifold and parameter uncertainties can be found in Reference [7].

Based on the identified set of points A on the manifold and the associated weightings calculated using Equation (8), the cumulative probability of all uncertain parameters can be obtained. Figure 4(a)–4(e) shows the cumulative probability for all uncertain parameters for both models M1 and M2. Table III summarizes the statistical properties (mean and coefficient

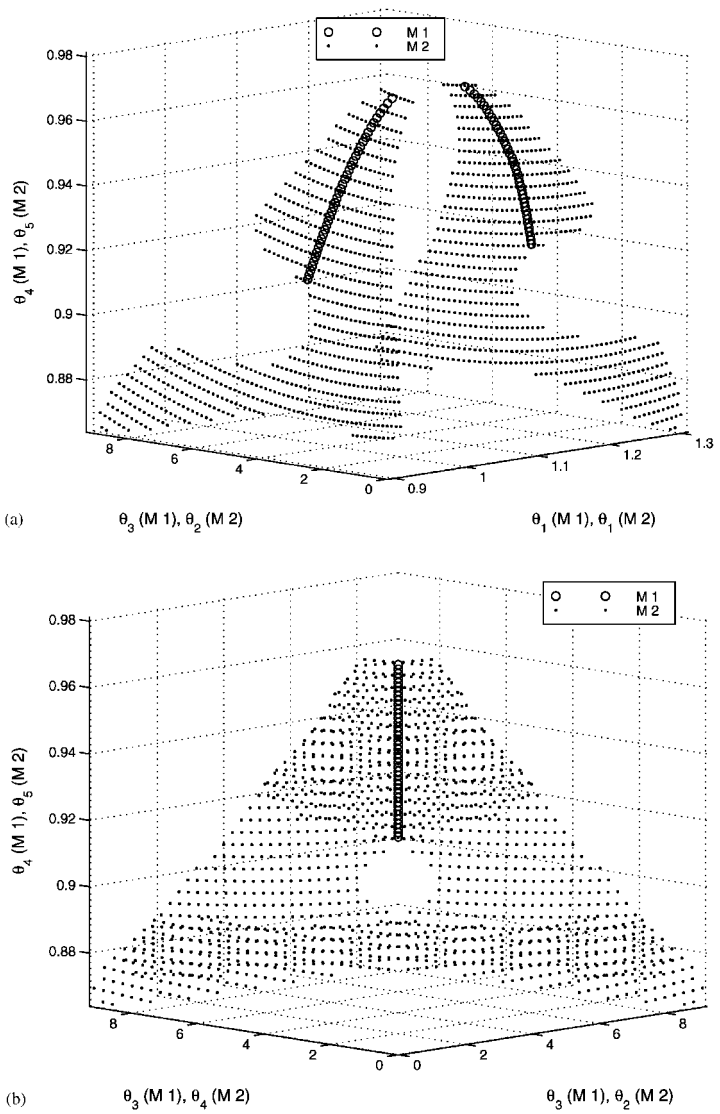

Figure 3. (a) Manifold in subspace A, (b) manifold in subspace B, and (c) manifold in subspace C.

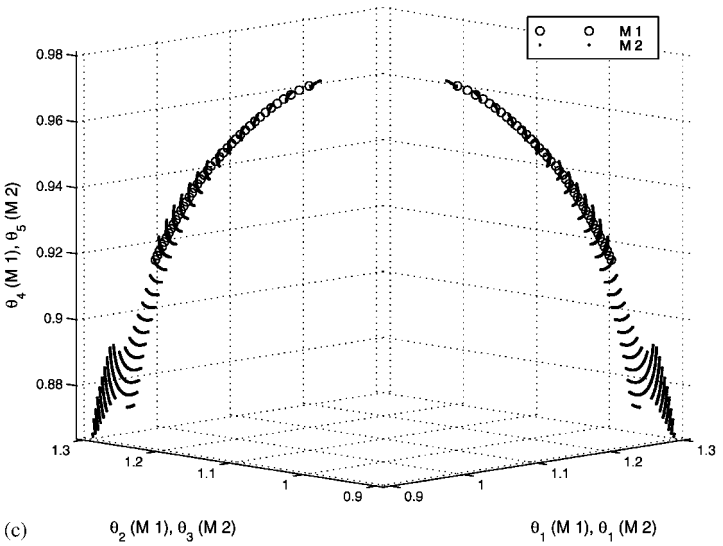

Figure 3. (Continued)

Table III. Mean and coefficient of variation for stiffness parameters.

	1-D manifold		2-D manifold	
	Mean	COV	Mean	COV
k_{yA}	1.0007	0.1003	1.0030	0.1034
k_{yE}	1.0007	0.1003	1.0030	0.1034
$k_{\theta A}$	1.1515	0.1751	1.2229	0.6218
$k_{\theta E}$	1.1515	0.1751	1.2231	0.6217
EI	0.9620	0.0063	0.9600	0.0093

of variation) of the stiffness parameters θ for the two models. Note that in general the uncertainty of θs for the two-dimensional manifold (M2) is higher than that for the one-dimensional manifold (M1).

Furthermore, the cumulative probability of maximum responses, such as maximum displacements and rotations at different nodes and maximum bending moments at both ends of the bridge were calculated. Figure 5(a)–5(c) show the cumulative probability of maximum displacement for nodes A, B and C for both models. Figures 6 and 7 show the cumulative probability of maximum rotation and bending moment, respectively, at node A. Table IV summarized the statistical properties (mean and coefficient of variation) of these maximum responses for both models. Once again, it is noted that, as with the uncertainty of θs, the uncertainty of maximum responses obtained from the two-dimensional manifold is higher than that obtained from the one-dimensional manifold.

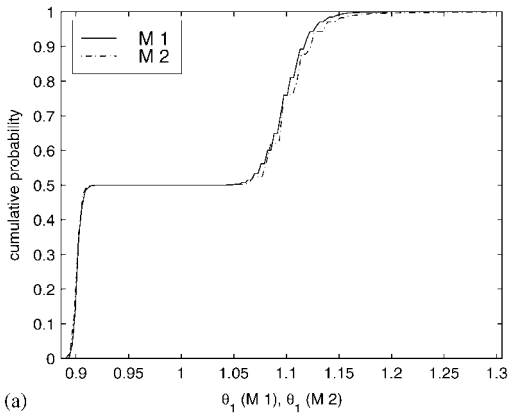

(a)

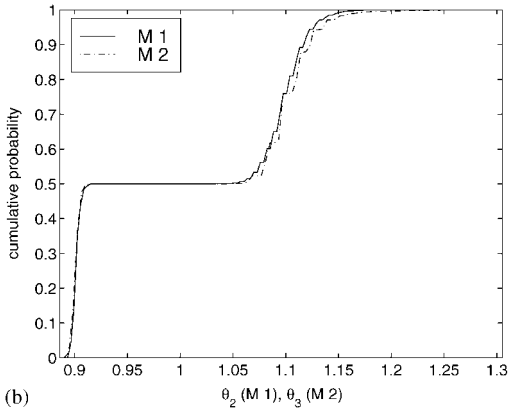

(b)

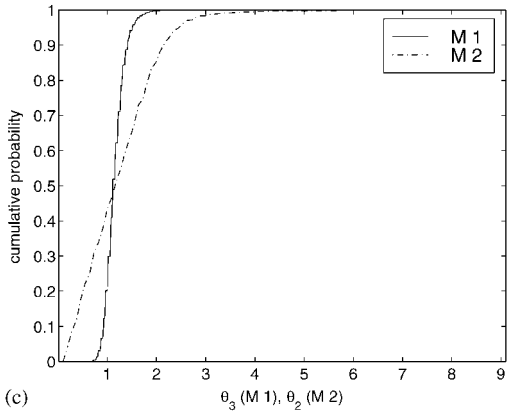

(c)

Figure 4. Cumulative probability of θ for translational spring at (a) node A, and (b) node E. Cumulative probability of θ for rotational spring at (c) node A and (d) node E. (e) Cumulative probability of θ for bending rigidity of the desk.

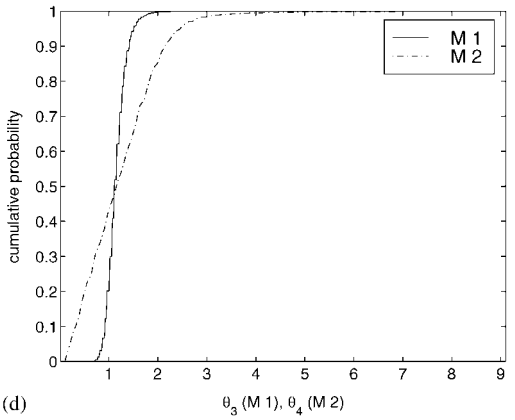

(d)

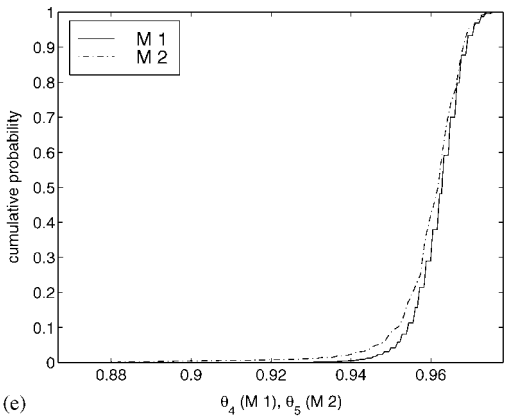

(e)

Figure 4. (Continued)

Table IV. Mean and coefficient of variation for maximum responses.

	1-D manifold		2-D manifold	
	Mean	COV	Mean	COV
Max. disp. at A	0.0115	0.1578	0.0115	0.1600
Max. disp. at B	0.0915	0.0031	0.0915	0.0050
Max. disp. at C	0.0073	0.0072	0.0073	0.0072
Max. rotation at A	0.0098	0.0071	0.0098	0.0123
Max. bending moment at A	20394	0.1750	21527	0.6097

5. CONCLUSION

The general Bayesian statistical framework presented in Reference [2] was extended to treat general unidentifiable cases. A new algorithm, referred to as the tangential-projection (TP)

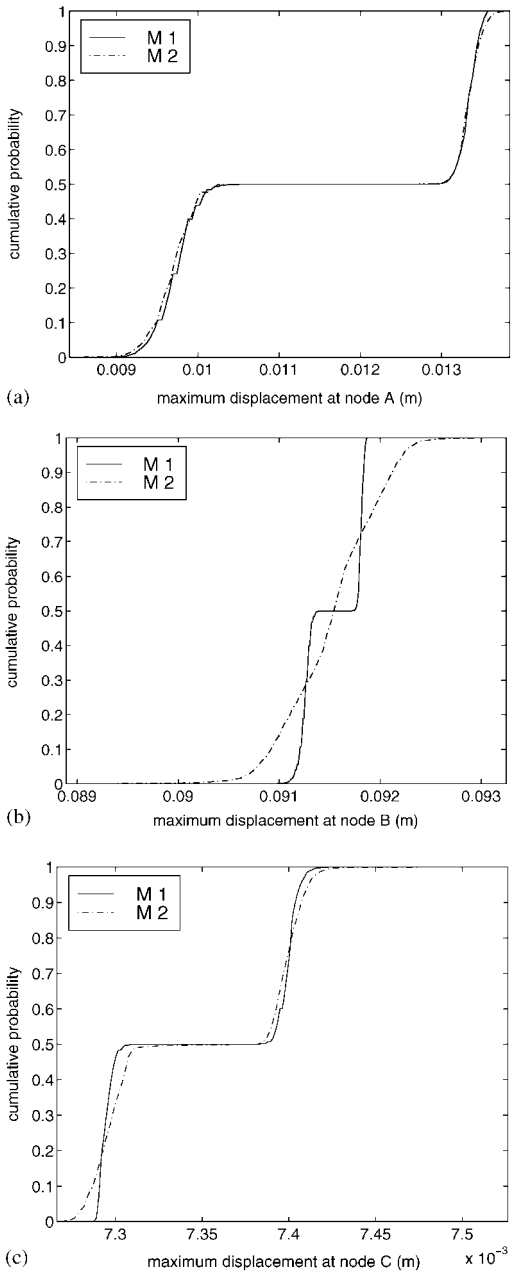

Figure 5. Cumulative probability of maximum displacement at (a) node A, (b) node B, and (c) node C.

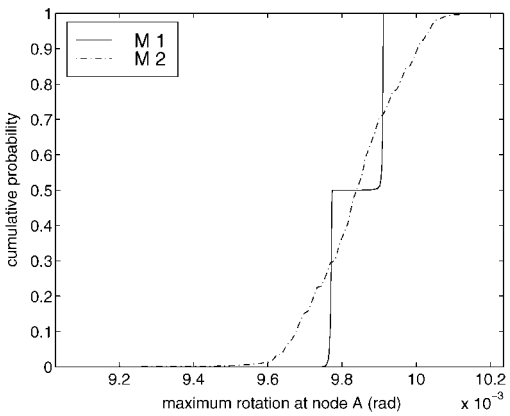

Figure 6. Cumulative probability of maximum rotation at node A.

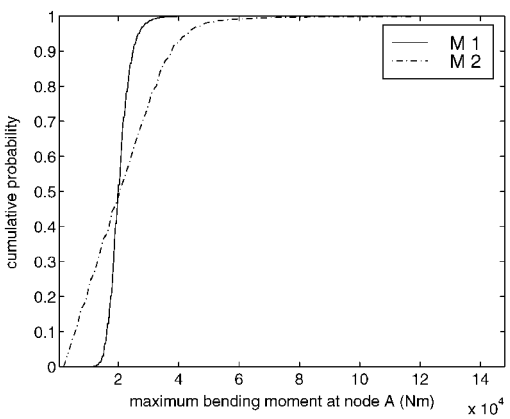

Figure 7. Cumulative probability of maximum bending moment at node A.

algorithm, for representation of the manifold of significant probabilities by a finite set of points was presented. This set of points, along with some appropriately calculated weightings, allows for the quantification of uncertainties of the model parameters and the predictive response. The TP algorithm is computationally significantly more efficient than the algorithm in Reference [6] as it efficiently builds the representative set of points by restricting the search for these points along only a small subspace of the parameter space extending only along the directions of the manifold. Furthermore, the algorithm offers a nearly uniformly spaced point generation and overcomes the difficulty encountered by the algorithm in Reference [6] in calculating the weightings for manifolds of dimension larger than one. The algorithm allows for the treatment of unidentifiable model updating problems that could not be resolved in the past.

ACKNOWLEDGEMENT

This work is based upon work partly supported by the Hong Kong Research Grant Council under grants HKUST 6041/97E and HKUST 6253/00. This support is gratefully acknowledged.

REFERENCES

1. Beck JL. Statistical system identification of structures. In *Proceedings 5th International Conference on Structural Safety and Stability*, ASCE, New York, 1989; 1395–1402.
2. Beck JL, Katafygiotis LS. Updating models and their uncertainties: Bayesian statistical framework. *Journal of Engineering Mechanics*, *ASCE* 1998; **124**(4):455–461.
3. Katafygiotis LS, Beck JL. Updating models and their uncertainties: model identifiability. *Journal of Engineering Mechanics*, *ASCE* 1998; **124**(4):463–467.
4. Lam Heung Fai. *Structural model updating and health monitoring in the presence of modeling uncertainties*. PhD thesis, Department of Civil Engineering, Hong Kong University of Science and Technology (HKUST), 1999.
5. Yang CM, Beck JL. Generalized trajectory methods for finding multiple extrema and roots of functions. *Journal of Optimization Theory and Applications* 1998; **97**(4):211–227.
6. Katafygiotis LS, Papadimitriou C, Lam HF. A probabilistic approach to structural model updating. *Soil Dynamics and Earthquake Engineering* 1998; **17**(7–8):495–507.
7. Katafygiotis LS, Lam HF, Papadimitriou C. Treatment of unidentifiability in structural model updating. *Advances in Structural Engineering* 2000; **3**(1):19–39.

